GAPS and Antideuterons

[General AntiParticle Spectrometer]

1303.3871, 1307.3538, 1303.0380

=> A measurement of atomic X-ray yields in exotic atoms and implications for an antideuteron-based dark matter search

=> The flight of the GAPS prototype experiment

Dark matter indirect searches: antiprotons, antideuterons

1. Source injection

- spectrum ~ R^{-2}
- abundances

2. Transport in the Galaxy

- diffusion: $R^{-\delta}$
- convection
- energy gains/losses
- fragmentation/decay

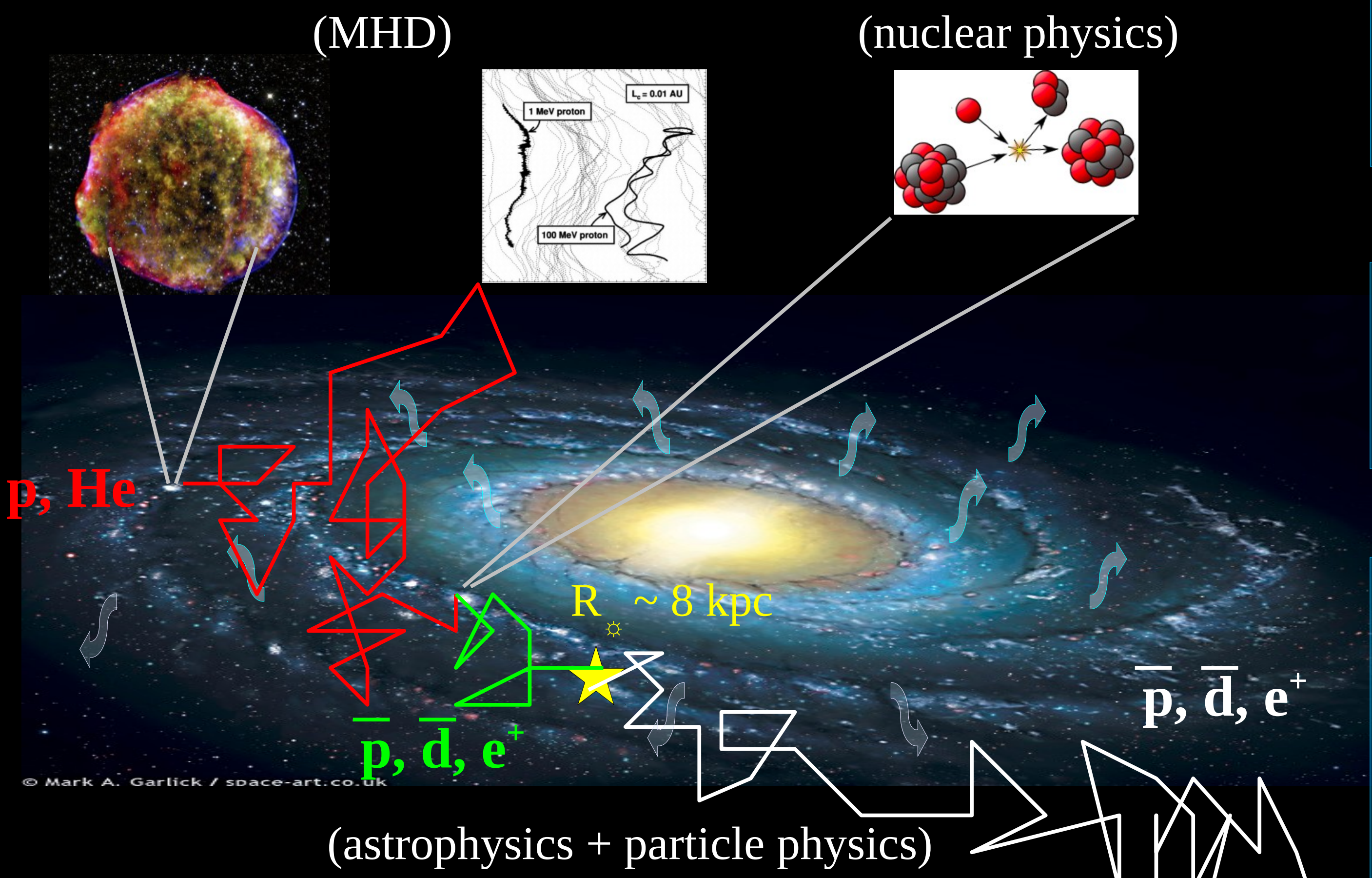

What about dark matter?

Universe (after Planck)

- 68.3 % dark energy
- 26.8 % dark matter
- 4.9 % ordinary matter

MilkyWay dark matter halo

- ~ spherical halo
- radius ~300 kpc

How to detect dark matter?

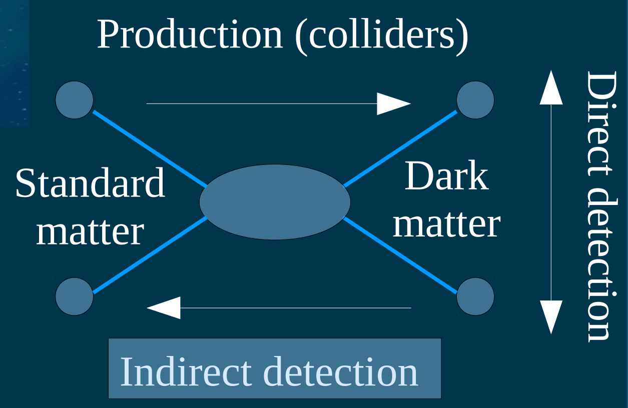

Approach followed:

→ Calibrate transport (model vs data): B/C, $^{10}Be/^{9}Be$
→ Calculate rare secondary fluxes (e^+, antiproton, antideuteron)
→ Excess from DM annihilation?

Best current limit on anti-deuterons

Fuke et al., PRL 95, 081101 (2005)

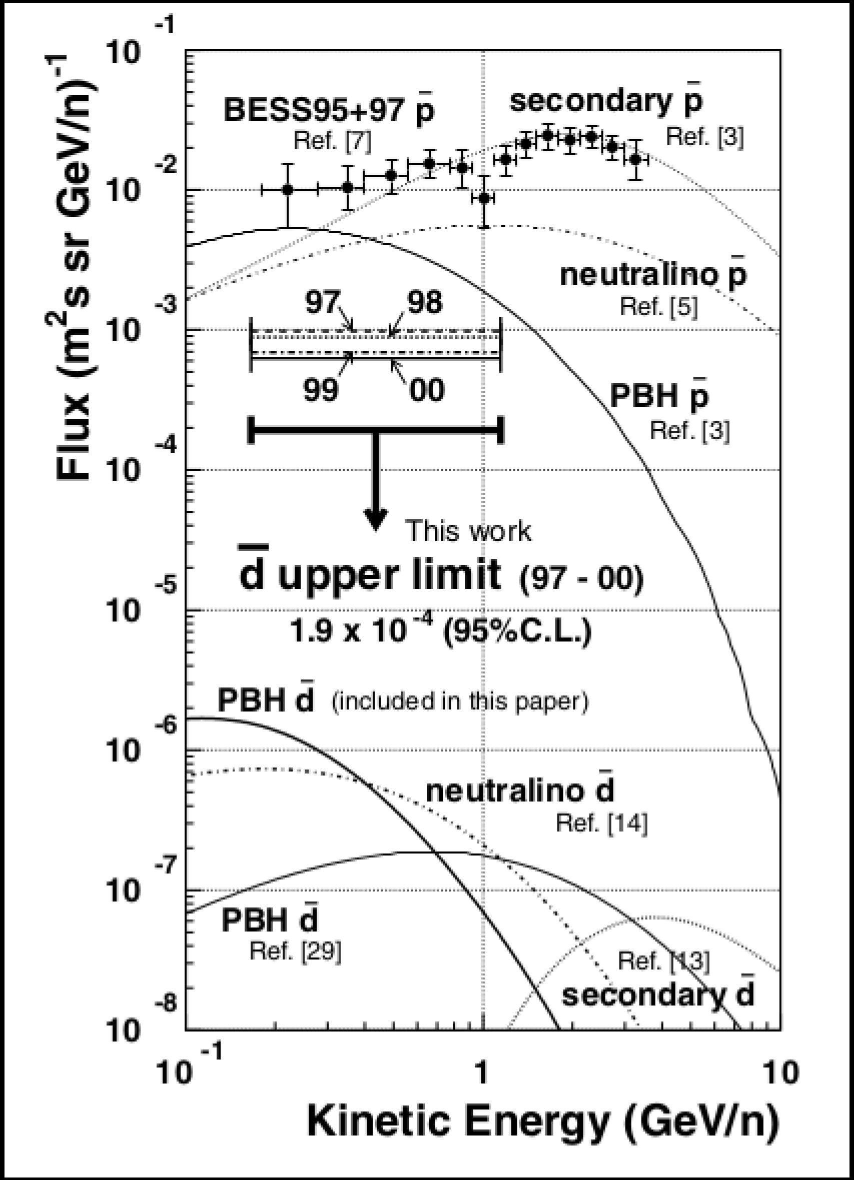

Foreseen limits from future experiments

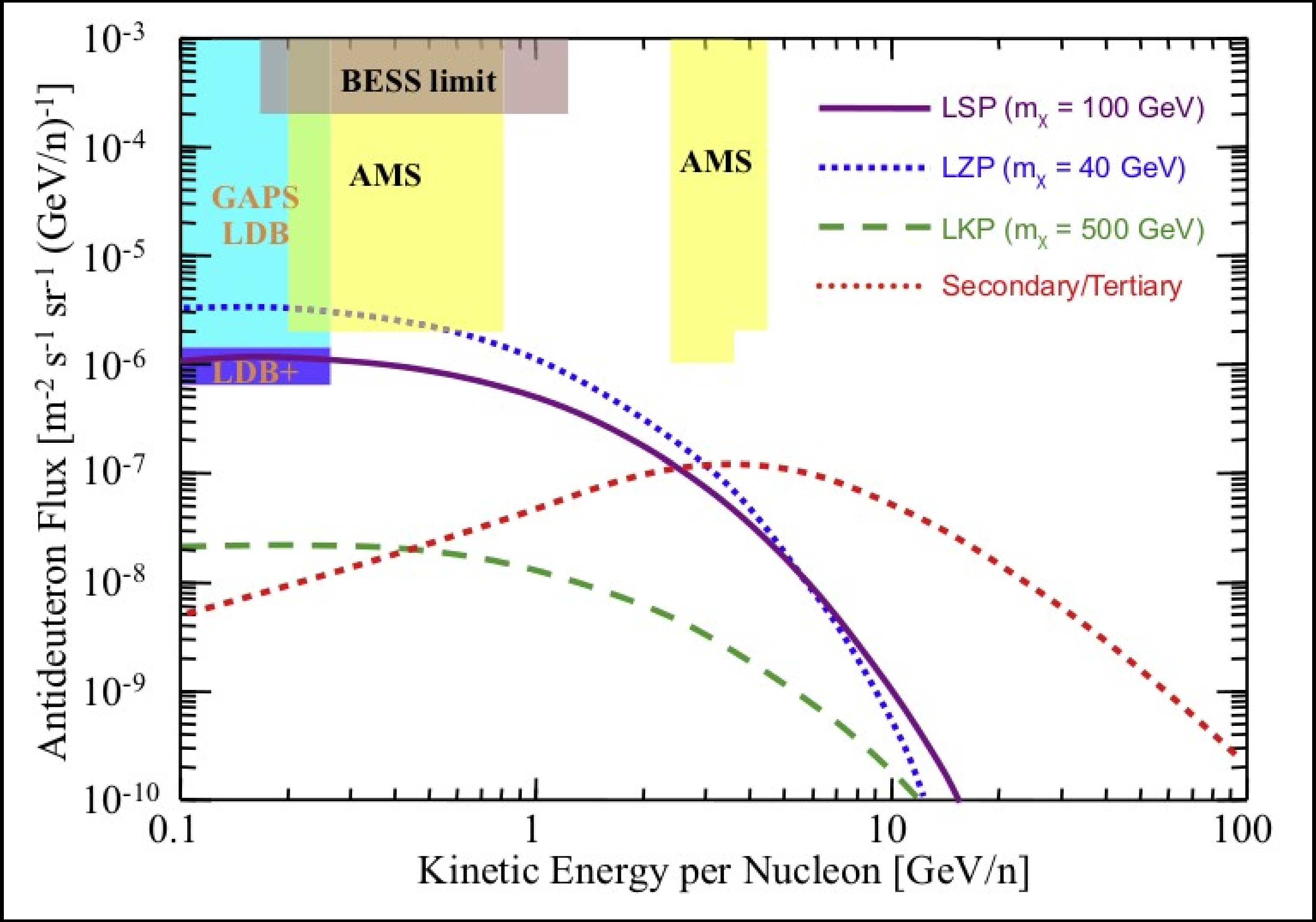

“Standard” CR detector (e.g., AMS-02)

[from N. Tomassetti’s talk]

Particles and nuclei are defined by their charge (Z) and energy (E ~ P)

TRD
Identify e+, e-

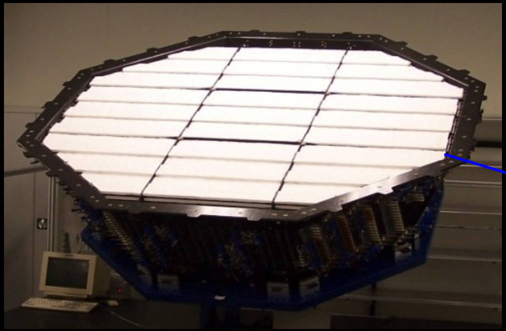

Silicon Tracker
Z, P

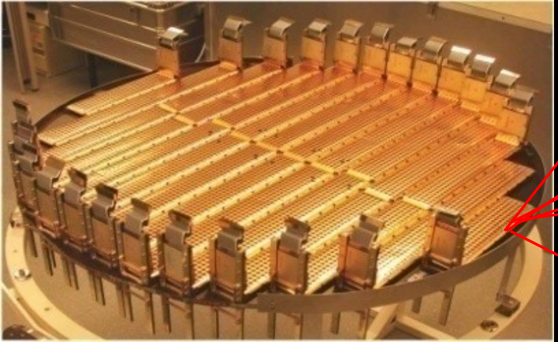

ECAL
E of e+, e-, γ

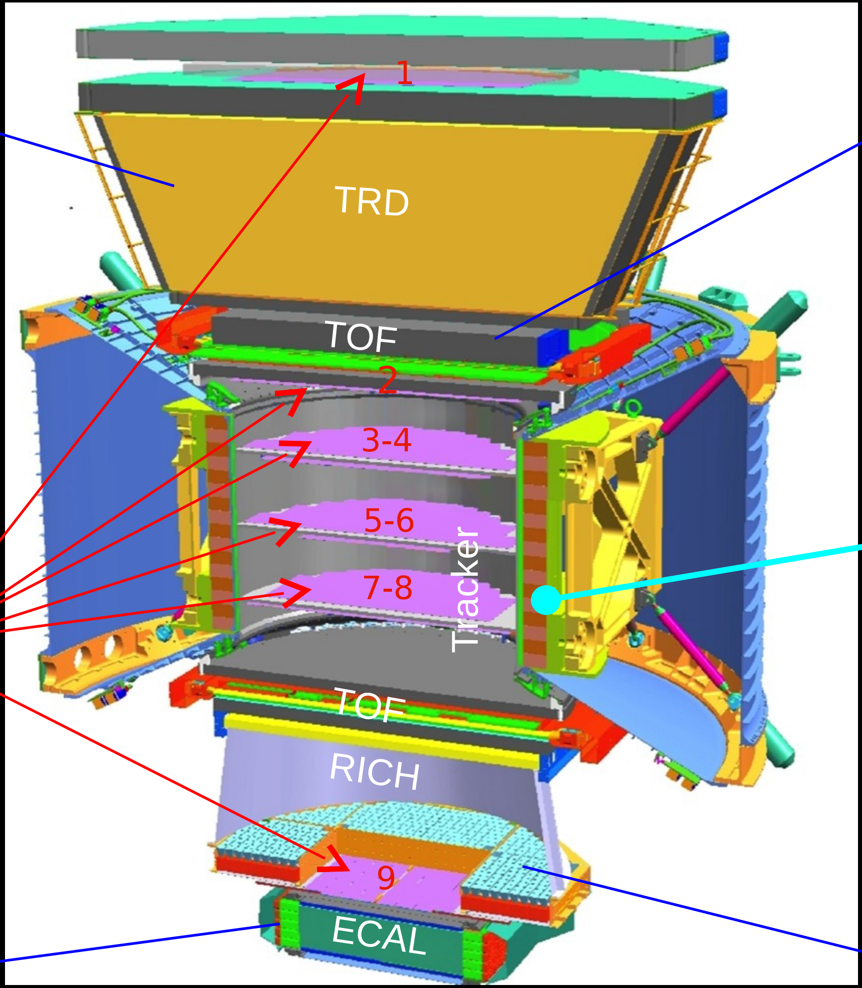

TOF
Z, E

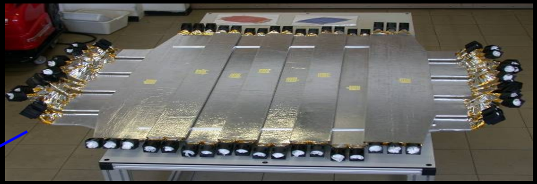

Magnet
±Z

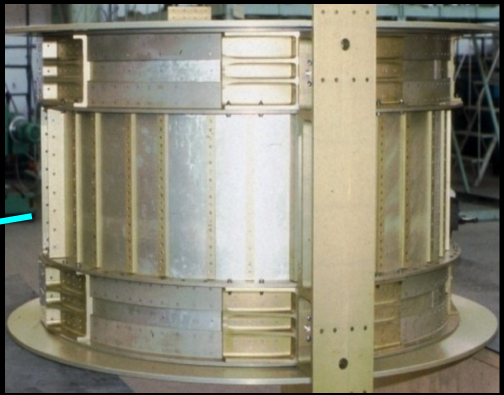

RICH
Z, E

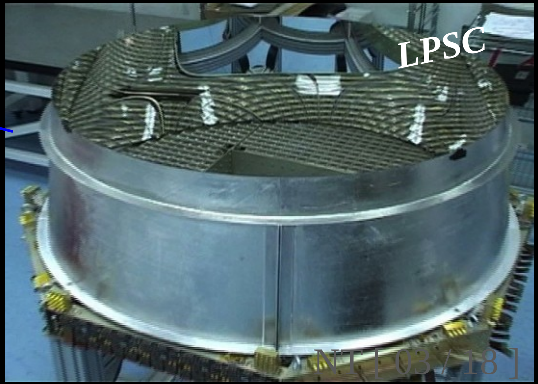

Z, P are measured independently from Tracker, RICH, TOF and ECAL

“Novel” technique: GAPS detector

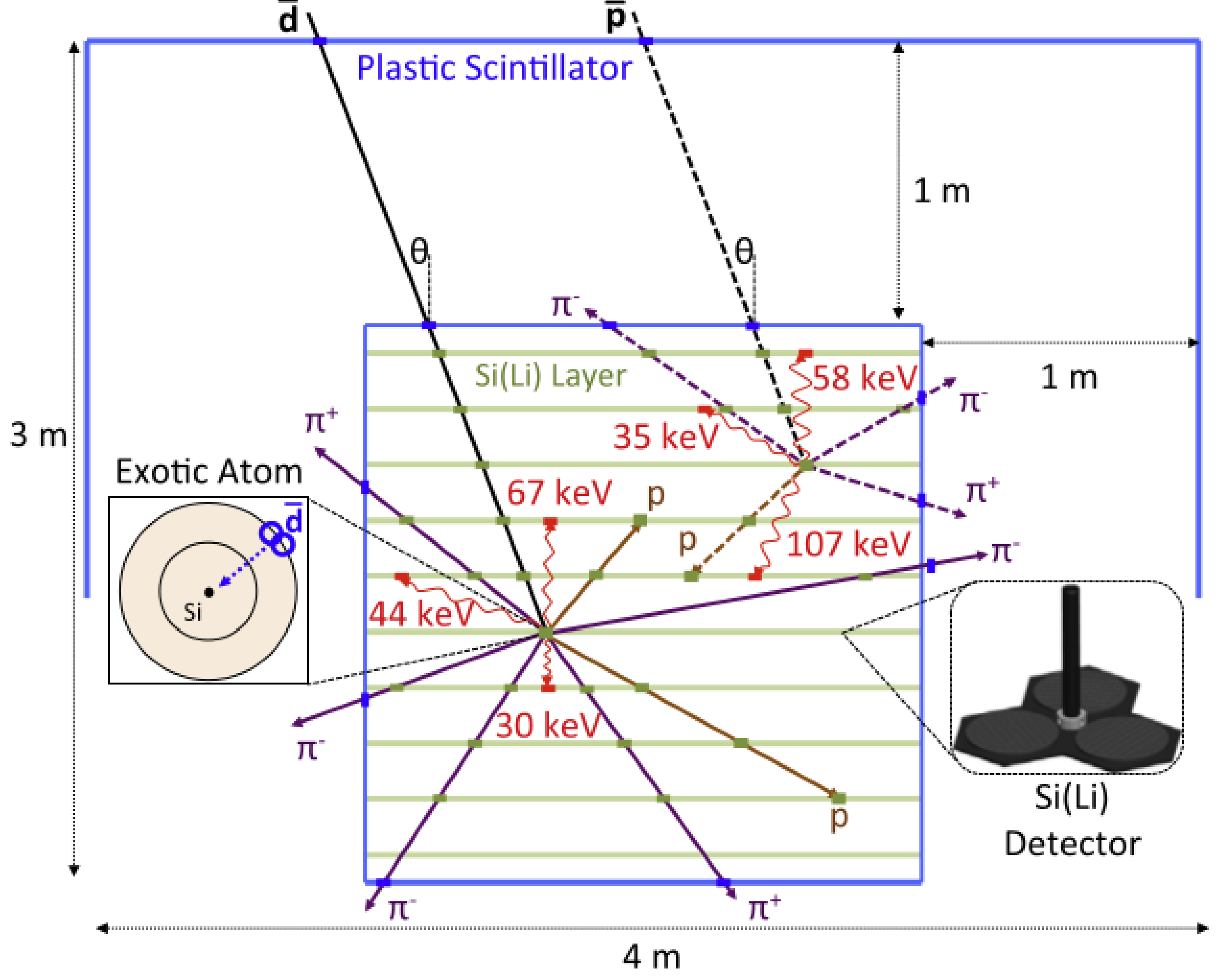

Fig. 2. The schematic view of the GAPS detector and the detection method. An antiparticle slows down and stops in the Si (Li) target forming an exotic atom. The atomic X-rays will be emitted as it de-excites followed by the pion and proton emission in the nuclear annihilation. The antideuteron identification method from antiprotons is also shown in the schematic view.

Cascade model and X-ray yields: MC calibration

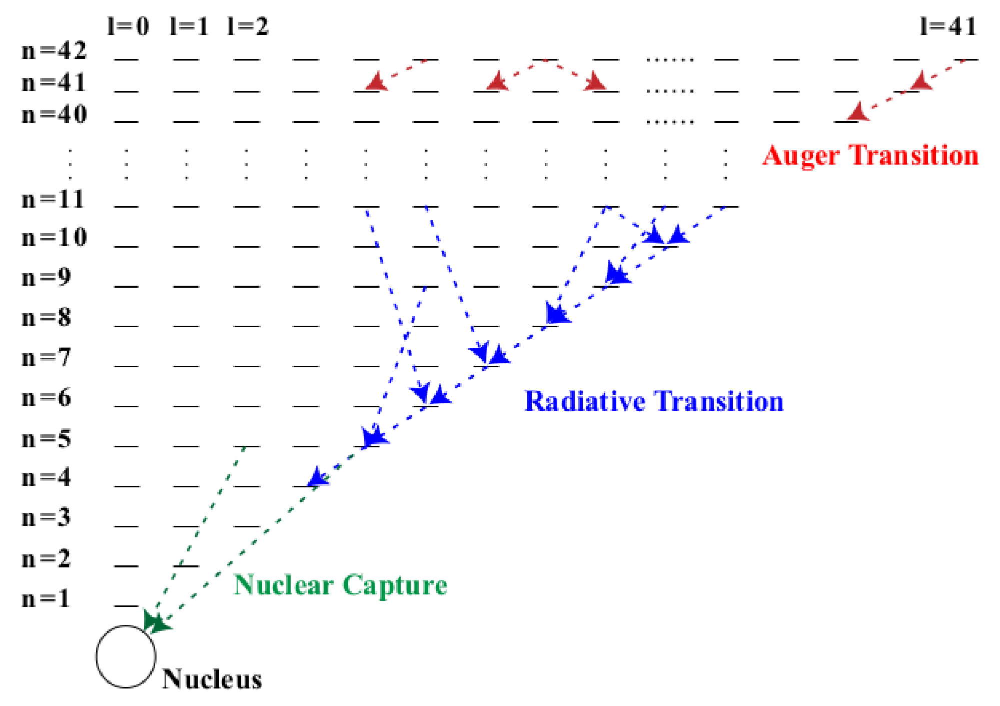

Fig. 3. The schematic view of the cascade model of the antiprotonic exotic atom. The Auger transitions dominate in high *n* states, while the radiative transitions dominate in low *n* states. The nuclear capture takes place in very low *n* states.

AUGER: In a high n state, an Auger electron is emitted as soon as the energy difference of the initial state (n1 ; l1) and the final state (n2 ; l2) exceeds the ionization energy

=> The transitions with $\Delta l = +/- 1$ dominate the process, due to the transition selection rules

Radiative Transition: increases as n decreases ($\Delta E_{n1\,;n2}$ increases), and becomes the main transition process in low n states.
=> High X-ray yield expected in the low n states

Nuclear Capture: Since the effective Bohr radius for the cascader is much smaller than the Bohr radius, the strong nuclear force interaction between the cascader and the nucleus can become large in low n states. This may terminate the deexcitation cascade of the exotic atom before it reaches the ground state, since the cascader is captured by the nucleus. In particular, the antiproton and the antideuteron annihilate with the nucleus due to the nuclear capture and produce pions and protons

Accelerator tests @ KEK (1)

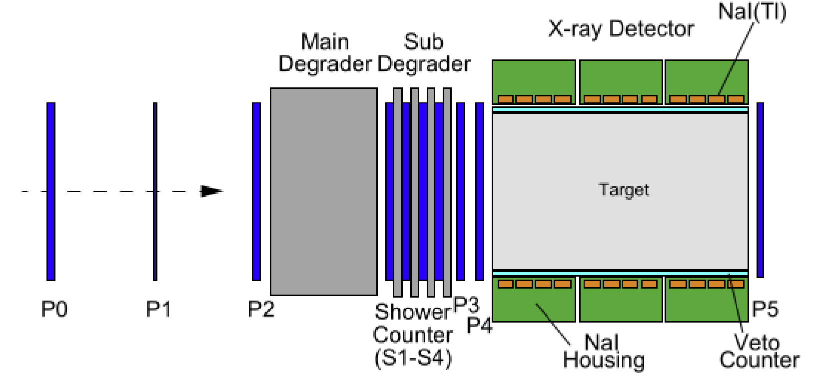

Fig. 5. The schematic view of the experimental setup at KEK in 2005. It was composed of a TOF system (P0-P5), degraders (lead brick and sheets), shower counters (S1-S4), a target and X-ray detectors. The distance between the P0 and P2 counters is 6.5 m and the overall length of the X-ray detector is ~ 50 cm.

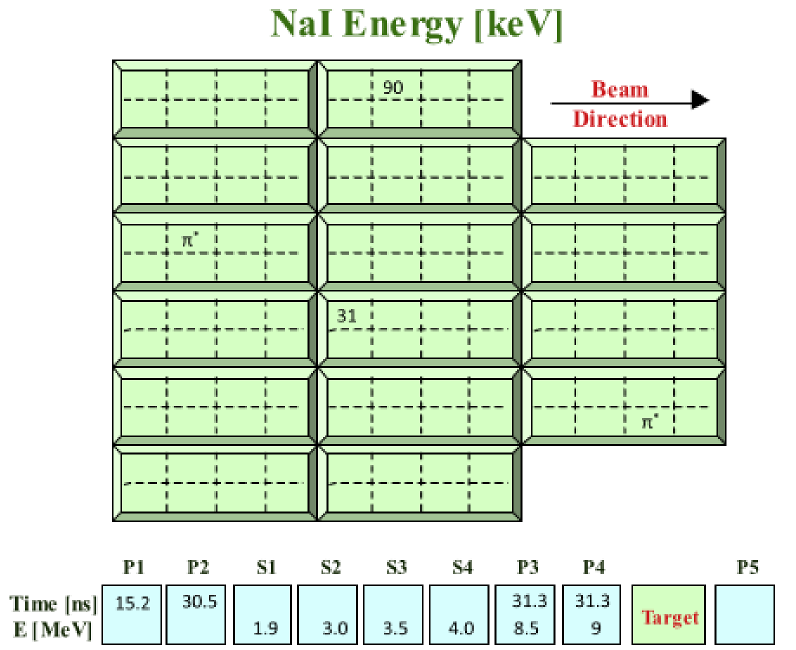

	P1	P2	S1	S2	S3	S4	P3	P4		P5
Time [ns]	15.2	30.5					31.3	31.3	Target	
E [MeV]			1.9	3.0	3.5	4.0	8.5	9		

Fig. 6. A typical antiproton event for the Al target. Numbers are the energy of the stopped X-rays and π^+ indicates a pion hit.

Accelerator tests @ KEK (2)

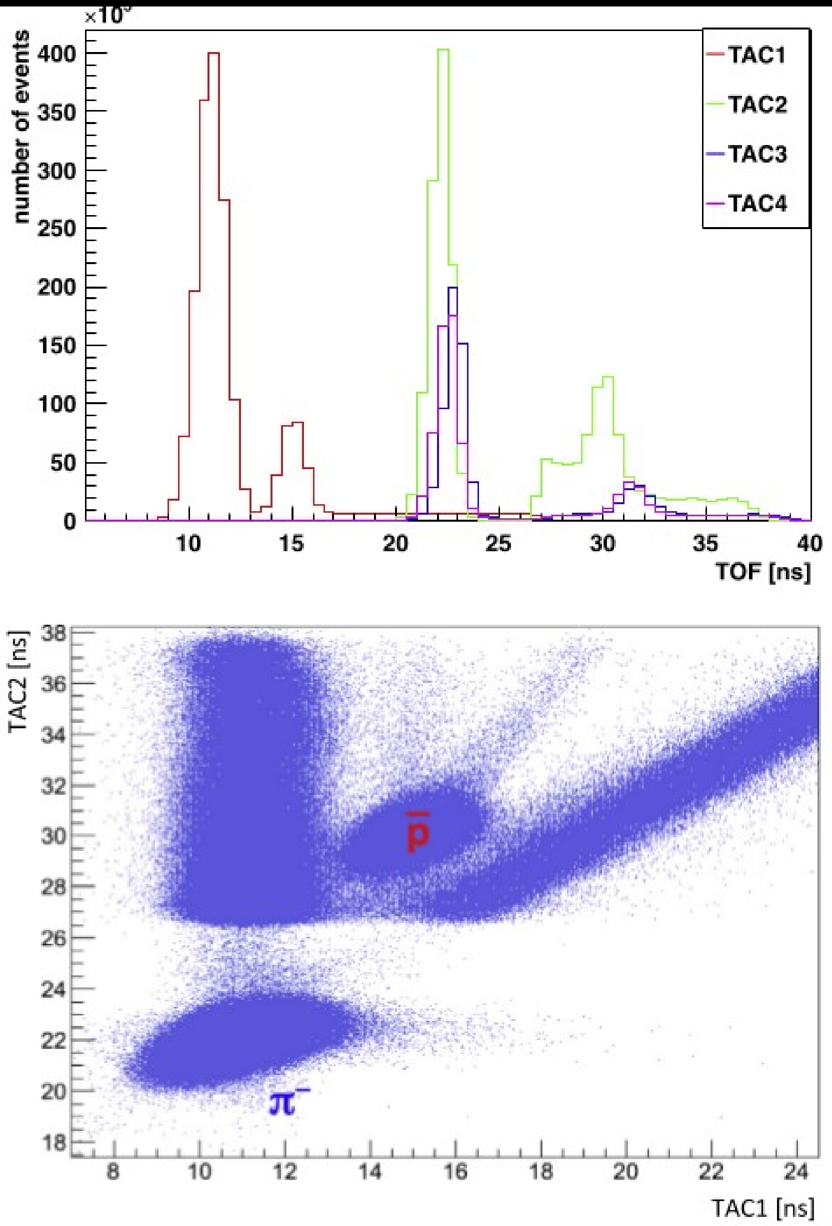

Fig. 9. TOF timing at TAC1 (red), TAC2 (green), TAC3 (blue), TAC4 (purple), and TAC1 vs. TAC2 (bottom). (For interpretation of the references to color in this figure legend, the reader is referred to the web version of this article.)

Accelerator tests @ KEK (3)

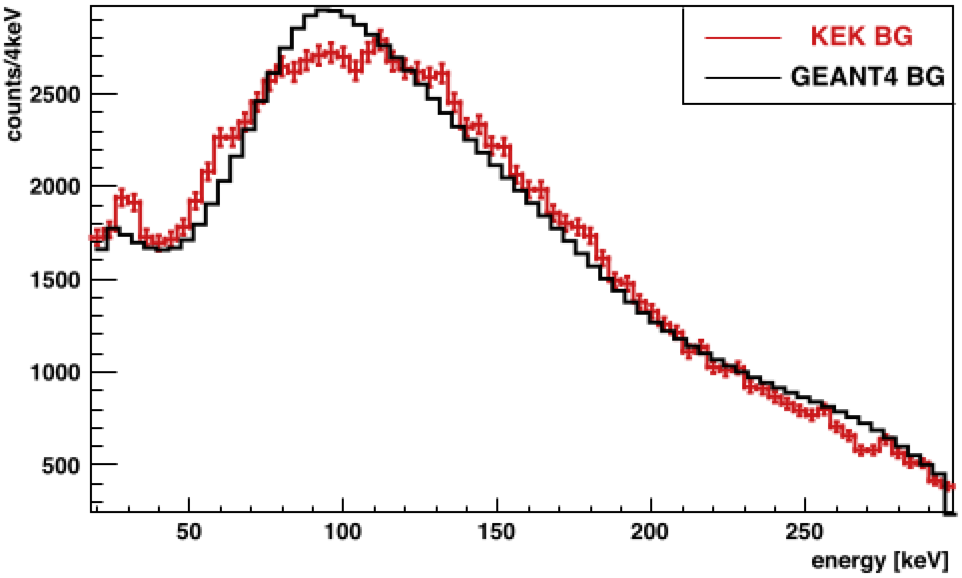

Fig. 11. The background models for the Al target obtained from the experime data (KEK BG) and the GEANT4 simulation (GEANT4 BG).

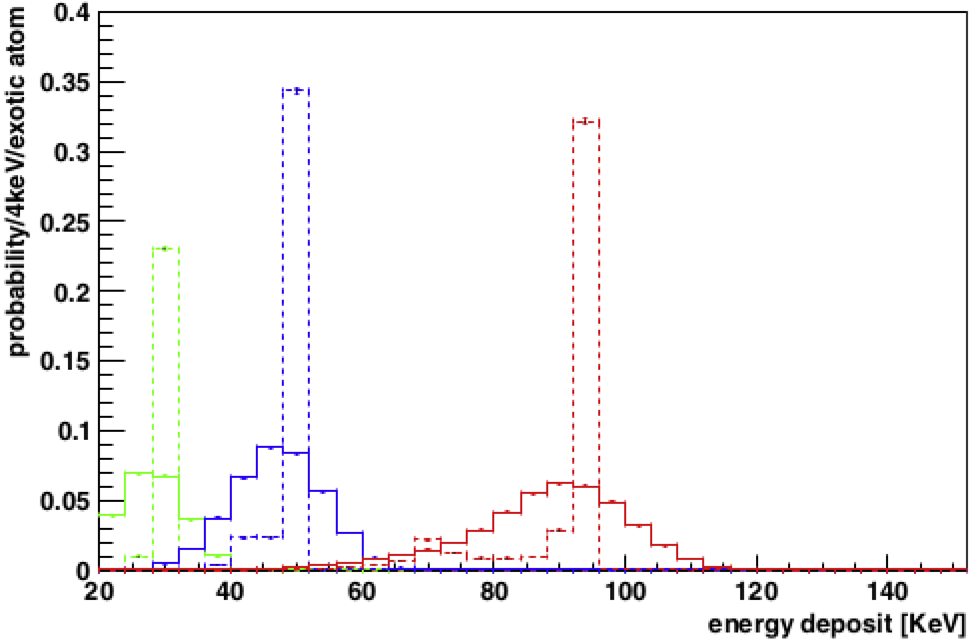

Fig. 12. Expected energy spectra in the detector for each atomic X-ray with the Al target. The green, blue, and red lines represent simulation results for 30 keV, 50 keV, and 92 keV X-rays, and the solid lines are the spectra with the detector response. It is normalized to the counts per exotic atom with 100% X-ray yield. (For

Accelerator tests @ KEK (4)

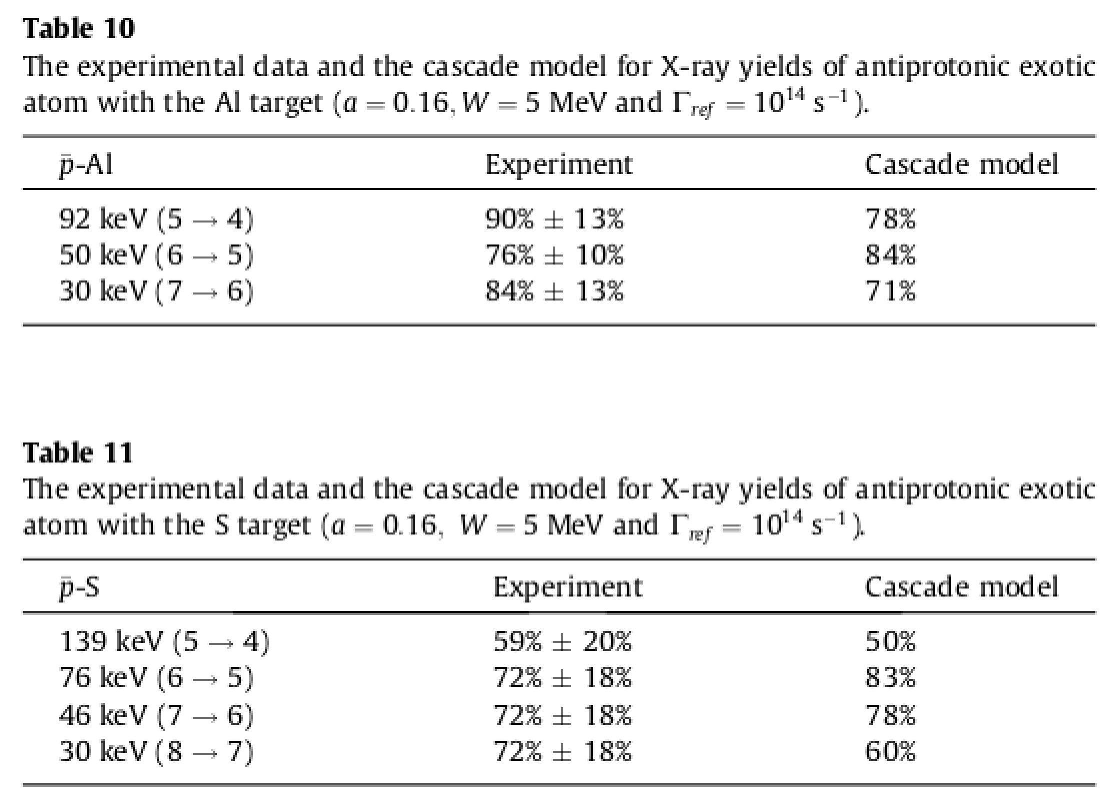

Table 10

The experimental data and the cascade model for X-ray yields of antiprotonic exotic atom with the Al target ($a = 0.16, W = 5$ MeV and $\Gamma_{ref} = 10^{14}\ \mathrm{s}^{-1}$).

$\bar{p}$-Al	Experiment	Cascade model
92 keV (5 → 4)	90% ± 13%	78%
50 keV (6 → 5)	76% ± 10%	84%
30 keV (7 → 6)	84% ± 13%	71%

Table 11

The experimental data and the cascade model for X-ray yields of antiprotonic exotic atom with the S target ($a = 0.16$, $W = 5$ MeV and $\Gamma_{ref} = 10^{14}\ \mathrm{s}^{-1}$).

$\bar{p}$-S	Experiment	Cascade model
139 keV (5 → 4)	59% ± 20%	50%
76 keV (6 → 5)	72% ± 18%	83%
46 keV (7 → 6)	72% ± 18%	78%
30 keV (8 → 7)	72% ± 18%	60%

Absolute X-ray yields for the antiprotonic exotic atom with Al and S targets were measured at KEK, Japan in 2005. The nuclear absorption was seen only in the very low n state for the S target. A simple but comprehensive cascade model has been developed to estimate the X-ray yields of the exotic atom. Since it is extendable to any kind of exotic atom (any negatively charged cascading particles with any target materials), the model was evaluated and validated with the experimental data and other models for the antiprotonic and muonic exotic atoms. The model allows us to estimate the X-ray yields of the antiprotonic and antideuteronic exotic atoms formed with any materials in the GAPS instrument and the X-ray yields for antiprotonic and antideuteronic exotic atoms with a Si target were estimated as ~ 80%. This is higher than previously assumed in [2], indicating the increase of the GAPS antideuteron sensitivity. The subsequent GAPS antideuteron sensitivity [3] indicates that the GAPS project has a strong potential to detect anti-deuterons produced by dark matter.

GAPS test flight (1)

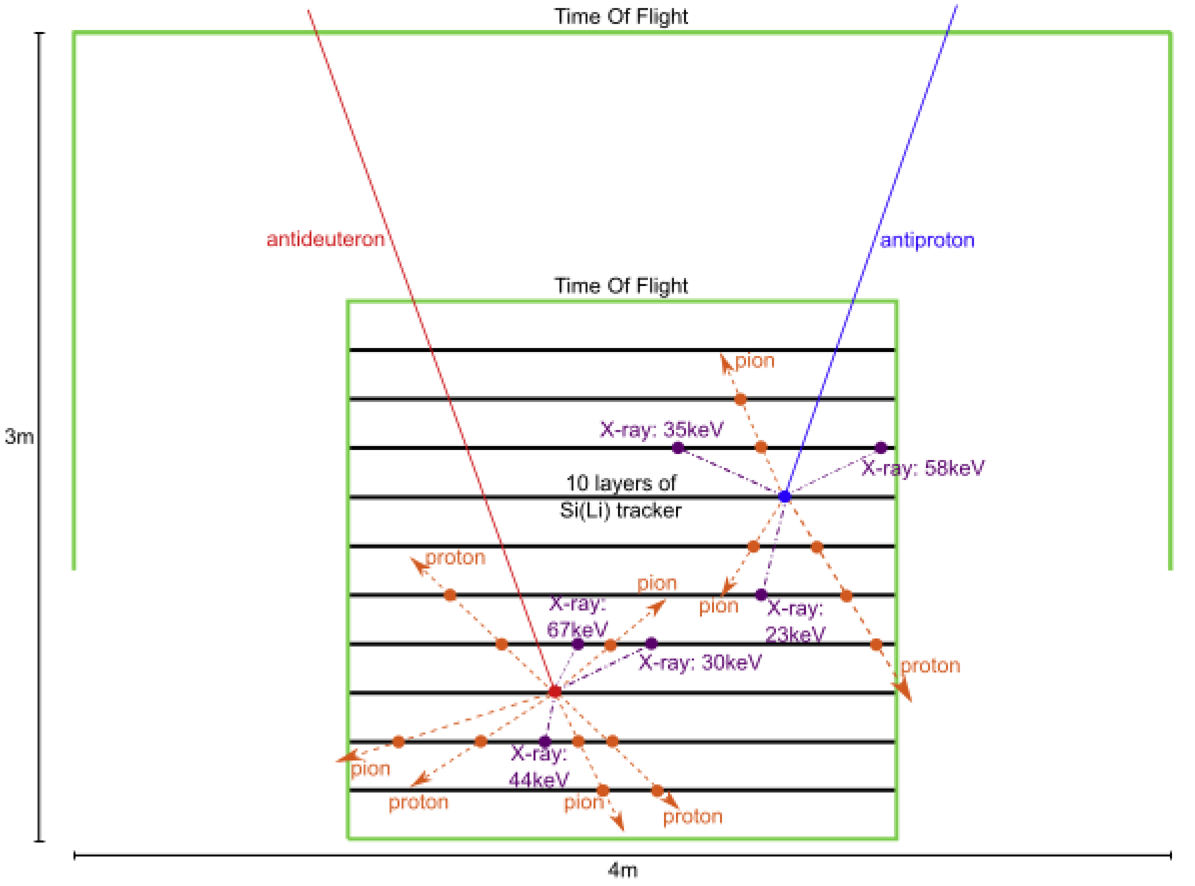

Fig. 2. GAPS detector concept with antiproton and antideuteron signatures.

GAPS test flight (2)

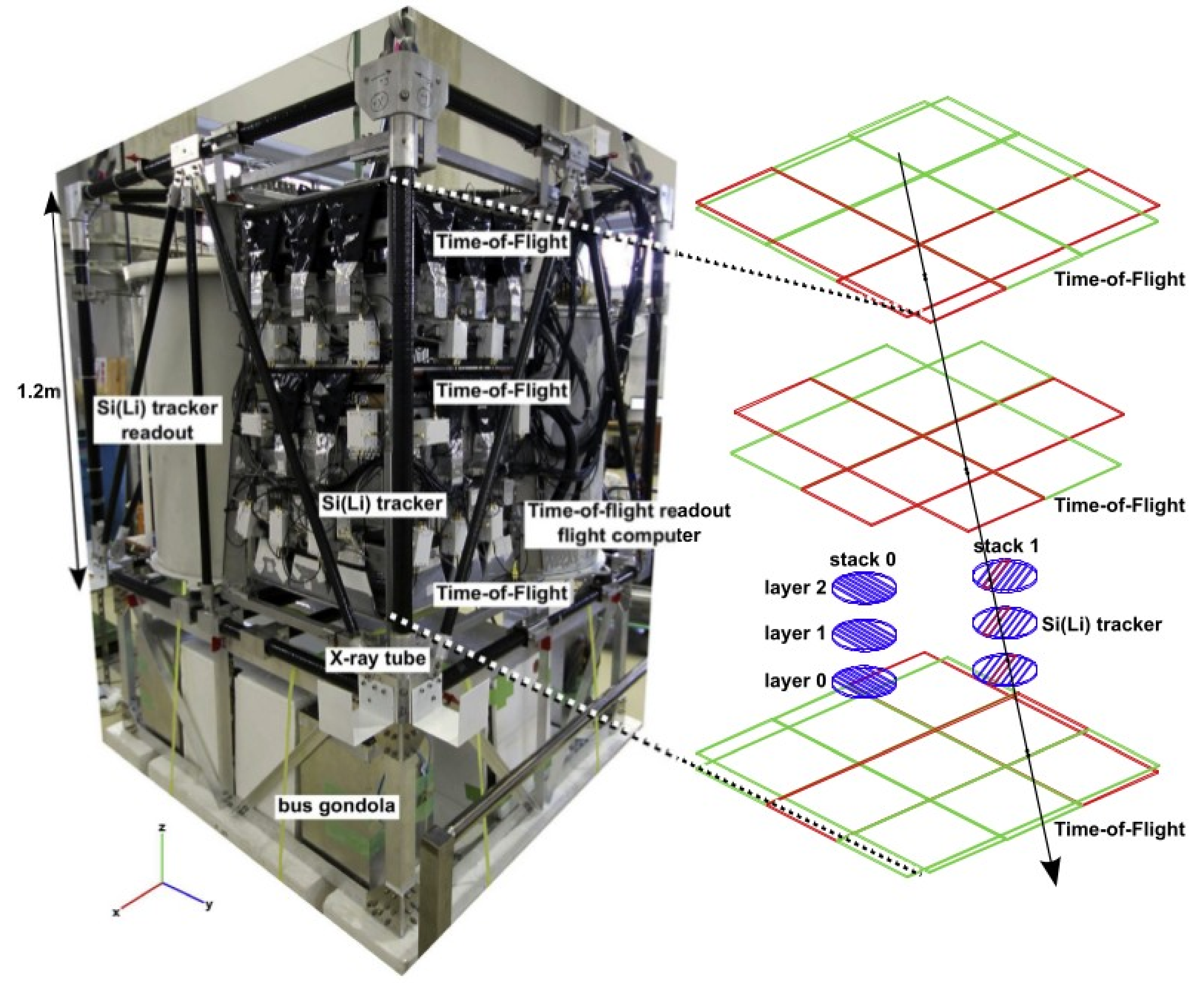

GAPS test flight (3)

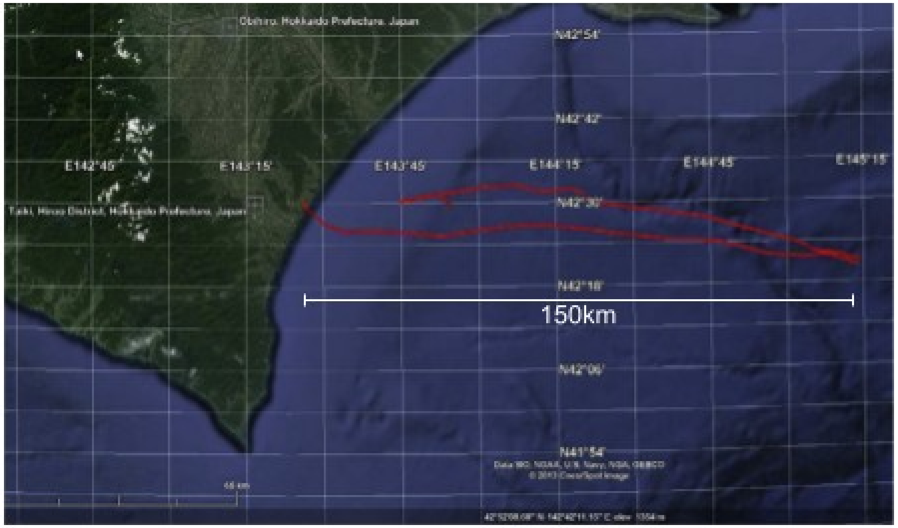

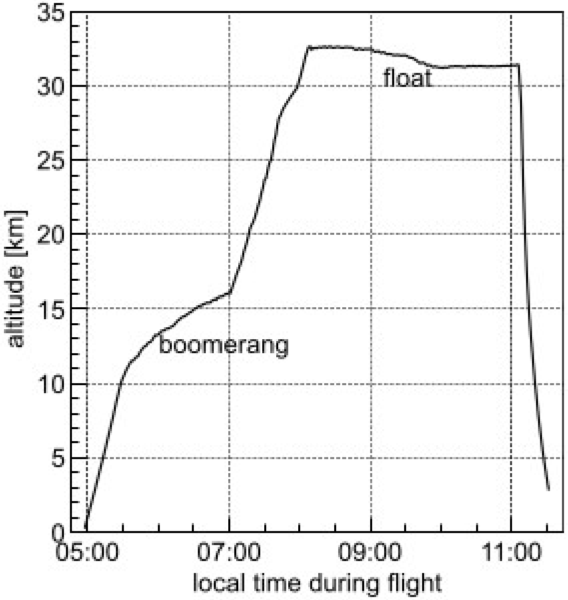

GAPS test flight (4)

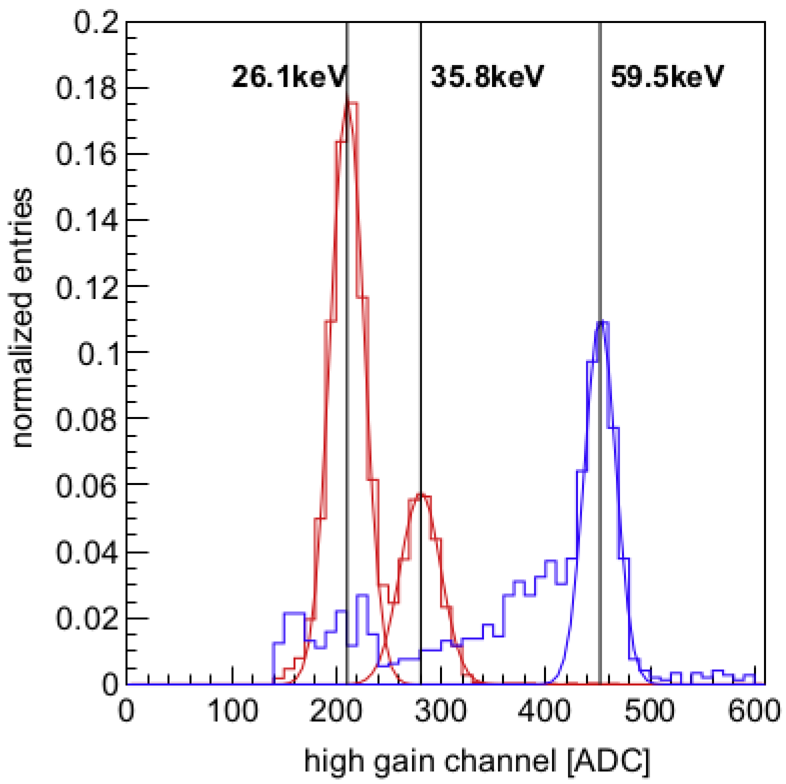

ig. 7. Calibration of one high gain channel with X-ray tube lines (red) and the 9.5 keV Am-241 line (blue) for one of the detectors in the middle tracker layer tack 0, layer 1, as defined in Fig. 3). (For interpretation of the references to color in his figure legend, the reader is referred to the web version of this article.)

GAPS test flight (5)

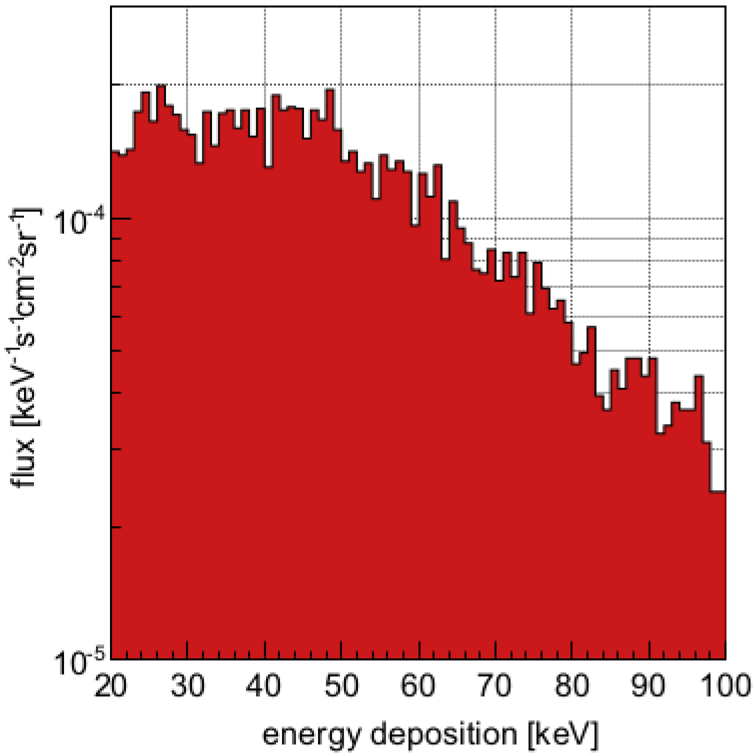

Fig. 15. X-ray flux during tracker trigger mode.

GAPS test flight (6)

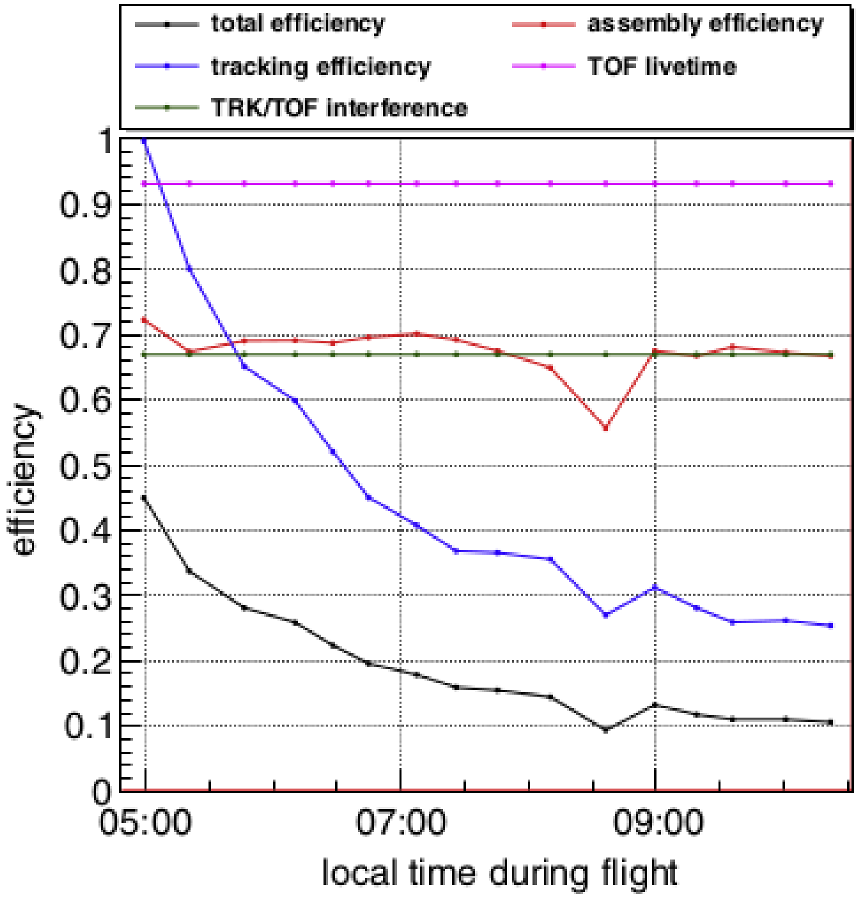

Fig. 26. Summary of correction factors for flux analysis as a function of flight time. The total efficiency (black) is the result of multiplying the assembly efficiency (red), the tracking efficiency (blue), the relative TOF livetime (magenta), and the TRK/TOF interference factor (green). (For interpretation of the references to color in this figure legend, the reader is referred to the web version of this article.)

GAPS test flight (7)

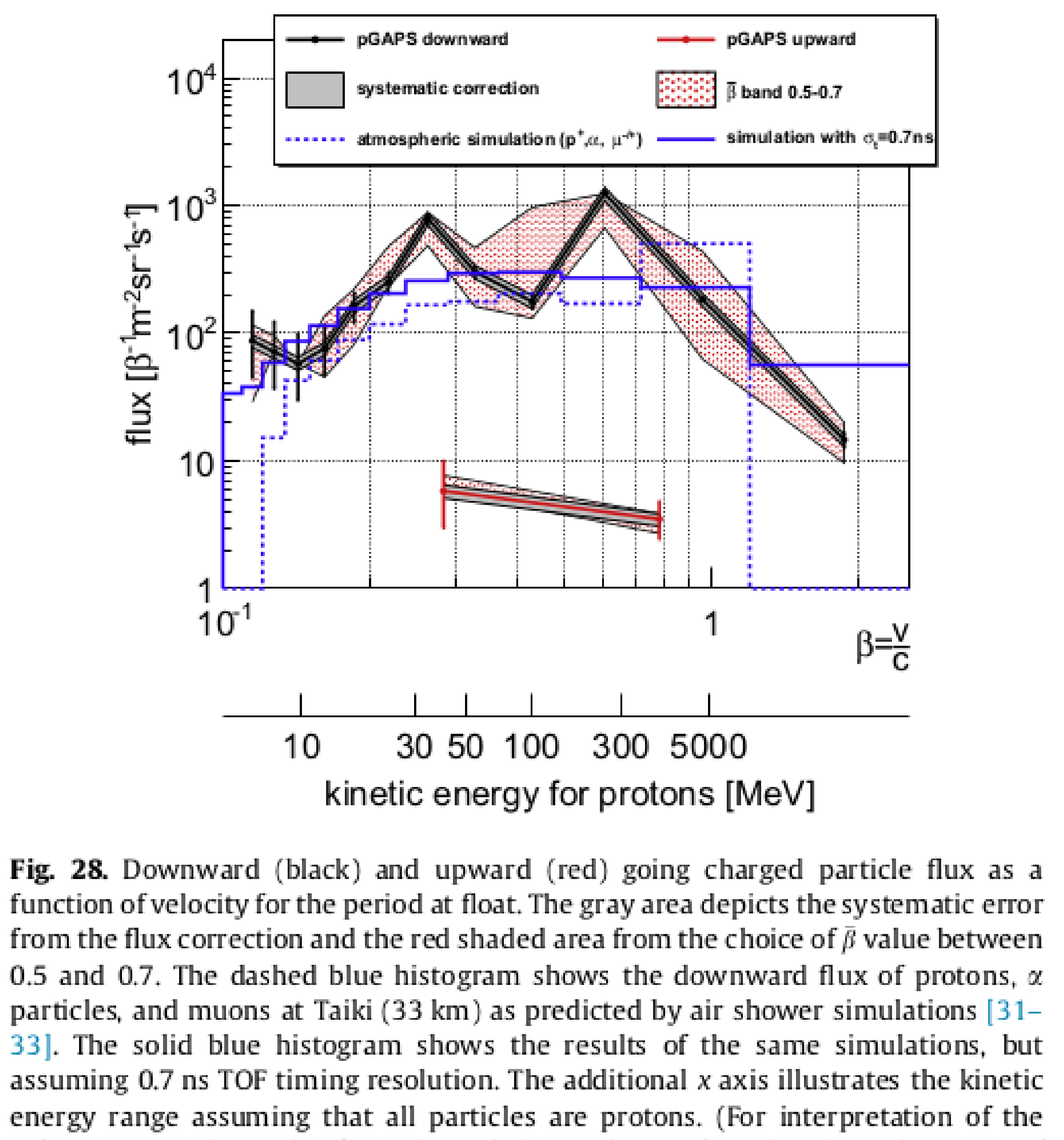

Fig. 28. Downward (black) and upward (red) going charged particle flux as a function of velocity for the period at float. The gray area depicts the systematic error from the flux correction and the red shaded area from the choice of $\bar{\beta}$ value between 0.5 and 0.7. The dashed blue histogram shows the downward flux of protons, α particles, and muons at Taiki (33 km) as predicted by air shower simulations [31–33]. The solid blue histogram shows the results of the same simulations, but assuming 0.7 ns TOF timing resolution. The additional x axis illustrates the kinetic energy range assuming that all particles are protons. (For interpretation of the

GAPS test flight: conclusions

The identification of dark matter is one of the most striking problems in physics and a low-energy cosmic ray antideuteron search has great potential in revealing deep insights. The GAPS experiment is specifically designed to perform this task. A prototype GAPS was successfully flown in June 2012. The purpose of this flight was to test and thoroughly analyze the concepts that form the basis for future flights. All goals for the flight were met and it was shown that the Si(Li) tracker detector modules and TOF worked reliably under flight conditions, the thermal model was verified [26], and background particle and X-ray fluxes were measured. The detailed design work for the full GAPS payload has been started already.